© 2017. Published by The Company of Biologists Ltd | Journal of Experimental Biology (2017) 220, 3916-3926 doi:10.1242/jeb.158543

RESEARCH ARTICLE

Metabolic costs imposed by hydrostatic pressure constrain bathymetric range in the lithodid crab *Lithodes maja*

Alastair Brown[1,§], Sven Thatje[1], James P. Morris[1,*], Andrew Oliphant[1,‡], Elizabeth A. Morgan[1], Chris Hauton[1], Daniel O. B. Jones[2] and David W. Pond[3]

ABSTRACT

The changing climate is shifting the distributions of marine species, yet the potential for shifts in depth distributions is virtually unexplored. Hydrostatic pressure is proposed to contribute to a physiological bottleneck constraining depth range extension in shallow-water taxa. However, bathymetric limitation by hydrostatic pressure remains undemonstrated, and the mechanism limiting hyperbaric tolerance remains hypothetical. Here, we assess the effects of hydrostatic pressure in the lithodid crab *Lithodes maja* (bathymetric range 4–790 m depth, approximately equivalent to 0.1 to 7.9 MPa hydrostatic pressure). Heart rate decreased with increasing hydrostatic pressure, and was significantly lower at ≥10.0 MPa than at 0.1 MPa. Oxygen consumption increased with increasing hydrostatic pressure to 12.5 MPa, before decreasing as hydrostatic pressure increased to 20.0 MPa; oxygen consumption was significantly higher at 7.5–17.5 MPa than at 0.1 MPa. Increases in expression of genes associated with neurotransmission, metabolism and stress were observed between 7.5 and 12.5 MPa. We suggest that hyperbaric tolerance in *L. maja* may be oxygen-limited by hyperbaric effects on heart rate and metabolic rate, but that *L. maja*'s bathymetric range is limited by metabolic costs imposed by the effects of high hydrostatic pressure. These results advocate including hydrostatic pressure in a complex model of environmental tolerance, where energy limitation constrains biogeographic range, and facilitate the incorporation of hydrostatic pressure into the broader metabolic framework for ecology and evolution. Such an approach is crucial for accurately projecting biogeographic responses to changing climate, and for understanding the ecology and evolution of life at depth.

KEY WORDS: Biogeographic range limitation, Heart rate, Metabolic theory, Respiration rate, Hydrostatic pressure, Hyperbaric physiology

INTRODUCTION

Depth range shifts are a typically overlooked response to changing climate, which may be as significant as geographic range shifts (Pinsky et al., 2013; Brown and Thatje, 2015; Deutsch et al., 2015). Accurately projecting the effect of climatic change on species' bathymetric distributions is impeded by uncertainty regarding the role of hydrostatic pressure (HP) in constraining bathymetric distribution in marine ectotherms, which is similarly typically ignored (Brown and Thatje, 2014, 2015; Deutsch et al., 2015). Bathymetric biodiversity patterns on deep continental margins appear driven by a physiological bottleneck imposed by the effects of high HP and low temperature on shallow-water organisms that colonised the deep sea following mass extinction events (Brown and Thatje, 2014). However, there has been no unequivocal demonstration of hyperbaric limitation of bathymetric range, and the mechanism limiting HP tolerance remains hypothetical (Brown and Thatje, 2014, 2015).

The physiological concept of oxygen- and capacity-limited thermal tolerance, where temperature tolerance is limited by capacity to supply sufficient oxygen to meet metabolic demand (Pörtner, 2010), has been proposed to apply to hyperbaric limitation (Brown and Thatje, 2014, 2015). This physiological concept has been integrated with fundamental principles of energy allocation and trade-offs developed in dynamic energy budget models to deliver a conceptual framework of environmental stress tolerance (Sokolova, 2013). This bioenergetic framework facilitates integration of the physiological effects of multiple environmental stressors, linking these effects to population-level consequences in the long term, and differentiating moderate environmental stress compatible with sustainable populations from high and extreme environmental stress limiting species distributions (Sokolova, 2013). Examining hyperbaric tolerance in the context of this framework offers the potential to identify the contribution of HP to bathymetric range limitation in marine organisms, and allow the fundamental effects of HP to be incorporated into the metabolic framework for ecology, which focuses on ecological effects on metabolic rate and consequent impacts on ecological processes at individual, population, community and ecosystem levels (Sibly et al., 2012). However, parameterising this model requires physiological data from sustained hyperbaric exposures at ecologically relevant temperatures in appropriate model taxa (Munro et al., 2015).

All lithodine king crabs share preference for cold-water environments, and their shallow-water geographic distribution appears to be constrained by the detrimental effects of temperature extremes (Hall and Thatje, 2009). Phylogenetic evidence also supports the hypothesis that lineage-specific physiological thresholds have recently differentiated lithodine genera in the colonisation of the deep sea: six of the 10 lithodine genera are restricted to depths shallower than 300 m in the North Pacific, the putative ancestral environment of the incipient lithodines, whilst the lithodine genera occurring deeper than 300 m (*Glyptolithodes*, *Lithodes*, *Neolithodes* and *Paralomis*) are distributed globally (Hall and Thatje, 2009). Submergence into the deep sea through an isothermal water column and subsequent global radiation

[1]University of Southampton, Ocean and Earth Science, European Way, Southampton SO14 3ZH, UK. [2]National Oceanography Centre, University of Southampton Waterfront Campus, European Way, Southampton SO14 3ZH, UK. [3]Scottish Association for Marine Science, Oban, Argyll PA37 1QA, UK. *Present address: Royal Belgian Institute of Natural Sciences, Rue Vautier 29, Brussels 1000, Belgium. ‡Present address: Institute of Biological, Environmental & Rural Sciences, Aberystwyth University, Penglais, Aberystwyth, Ceredigion SY23 3FG, UK.

*Author for correspondence (alastair.brown@noc.soton.ac.uk)

A.B., 0000-0002-2126-203X

Received 21 February 2017; Accepted 5 September 2017

Journal of Experimental Biology

Journal of Experimental Biology (2017) 220, 3916-3926 doi:10.1242/jeb.158543

are proposed to result from ecological adaptation (Hall and Thatje, 2009).

The northern stone crab *Lithodes maja* (Linnaeus 1758) is distributed from 38°N along the North American coast to Newfoundland, across to the west and east coasts of Greenland, the coasts of Iceland, and down the Norwegian coast to the British Isles and the Netherlands, with a bathymetric distribution of 4–790 m (Zaklan, 2002; OBIS, 2016). Acute hyperbaric tolerance of *L. maja*'s early development extends beyond the known bathymetric distribution of the species, but demonstrates an ontogenetic decrease that approaches the species' depth limit, suggesting that adult hyperbaric tolerance may influence bathymetric distribution in *L. maja* (Munro et al., 2015). Therefore, the aim of this study was to use *L. maja* as a model organism to determine: (1) mechanisms limiting hyperbaric tolerance, and (2) whether the adult critical hyperbaric threshold coincides with the species depth distribution limit. We investigated physiological effects of HP in *L. maja* to test the hypothesis and ecological relevance of oxygen- and capacity-limitation in hyperbaric tolerance. Integration of physiological processes across organisational levels may deliver insight into mechanisms underlying responses to stressors (Cottin et al., 2012; Morris et al., 2015c; Munro et al., 2015). Consequently, multiple physiological measures were examined to reveal both systemic and cellular challenges and responses during hyperbaric exposures.

Heart rate in malacostracan crustaceans is regulated by extrinsic neuronal and hormonal factors, and has been used as a proxy for respiration and a sensitive indicator of physiological impairment (Frederich and Pörtner, 2000). However, respiration is defined by complex dynamics: heart rate is only one aspect. Cardiac output is also affected by the amplitude of each beat, which can vary independently of heart rate (McMahon, 1999; Wilkens, 1999). Systemic haemolymph distribution may be altered by selective allocation of cardiac output (Wilkens, 1999) and the partial pressure gradient driving oxygen diffusion across gaseous exchange sites may be adjusted by modification of haemocyanin–oxygen binding properties (Bridges, 2001). Consequently, metabolic rate is often assessed as an alternative indicator of environmental tolerance (Frederich and Pörtner, 2000). Metabolic rate is the fundamental biological rate: the rate of energy uptake, transformation and allocation (Brown et al., 2004). Because energy is obtained by oxidising carbon compounds, aerobic metabolic rate is equivalent to the rate of aerobic respiration (Brown et al., 2004). Maintenance costs are measured as standard or basal metabolic rate (Kooijman, 2010). Measuring metabolic rate accurately and consistently is challenging (Brown et al., 2004), but the fixed stochiometry of respiratory gas exchange means that it is nearly as accurate and more practical to measure the rate of oxygen consumption (Withers, 1992). Therefore, both heart rate and oxygen consumption were measured during experimental treatments.

The most widely studied genetic marker of hyperbaric stress physiology in marine invertebrates is the 70 kDa heat-shock protein family (HSP70) (Cottin et al., 2012; Morris et al., 2015a,b,c; Munro et al., 2015). Heat-shock proteins are molecular chaperones and upregulation of the *hsp70* gene signifies alteration of proteins' native conformation (Morris et al., 2013), which may result from elevated HP (Cottin et al., 2012; Morris et al., 2015a,b,c; Munro et al., 2015). However, such generalised stress markers are involved in the ubiquitous cellular stress response and are highly reactive to a multitude of potential stressors; therefore, interpreting shifts in transcription may be challenging (Morris et al., 2013). In contrast, the *cs* gene codes for the enzyme citrate synthase, which is a key and rate-limiting constituent of the tricarboxylic acid (TCA) cycle (Goldenthal et al., 1998). The expression of the *cs* gene has recently been shown to correlate with mitochondrial citrate synthase activity (Basse et al., 2015; Stager et al., 2015), which may be elevated at high HP (Brown and Thatje, 2014). Similarly, the *α-tubulin* gene codes for subunits of α-tubulin microtubules, which are essential cytoskeletal components affecting cell division in all eukaryotes and reflect cell cycling (Nogales, 2000), which may be arrested at high HP (Brown and Thatje, 2014). Increased transcription of the *narg* gene, which codes for an *N*-methyl-D-aspartate (NMDA) receptor-regulated protein, has been identified as a hyperbaric neurophysiological stress marker (Morris et al., 2015a,b,c; Munro et al., 2015). NMDA receptors are ligand- and voltage-gated glutamate receptors: ion channels that mediate excitatory neurotransmission (Dingledine et al., 1999), which may be impeded at high HP (Brown and Thatje, 2014).

Acclimation to low temperature and high HP is proposed to include integrated homeoviscous modifications in membrane lipid saturation (Pörtner, 2002), with unsaturation of fatty acids required to maintain membrane function under low temperature and/or high HP (Somero, 1992; Hazel, 1995). Shifts in phospholipid fatty acid composition indicate a cellular response to counteract low-temperature- and/or HP-induced decrease in membrane fluidity and permeability (Somero, 1992; Hazel, 1995), which limits the movement of molecules across membranes and affects cell signalling (Hazel and Williams, 1990). In contrast, lactate accumulation in crustacean haemolymph represents increasing systemic reliance on anaerobic metabolism (Booth et al., 1982).

MATERIALS AND METHODS

Sample collection, transfer and maintenance

Adult specimens of *L. maja* were collected using baited traps, from ∼60 m depth in Gullmarsfjord, Sweden. Active specimens without extensive necrosis or externally visible parasites were maintained in an open aquarium system at the Sven Lovén Centre for Marine Sciences – Kristineberg (seawater from a 30 m deep intake; salinity 35, temperature 6–10°C, natural light cycle) for several weeks prior to relocation to the National Oceanography Centre Southampton (NOCS). Animals were starved for 3 days prior to relocation to reduce the potential for adverse specific dynamic action effects. Specimens were isolated in polystyrene boxes lined with towels wetted with seawater, and transported in a temperature-controlled van (6°C; <24 h). Specimens were transferred to a recirculating aquarium (1 µm filtered seawater: salinity 32.7, temperature 6°C; 24-h darkness) immediately upon arrival at the NOCS. Maintenance temperature was selected to match the temperature in the field at the time of sampling. Animals were fed squid (*Nototodarus sloanii*) mantle weekly; unconsumed food was removed after 24 h. Animals continued to thrive under maintenance conditions. Feeding, moulting, competition for mates, mating, and larval release and development to juvenile were all observed post-transfer. However, animals for experimental treatments were sampled and transported on several occasions (October 2011, April 2012 and June 2013) to reduce the potential for experimental confounding by adverse effects of long-term aquarium maintenance. In each case transportation survival was >90%. Animals were used in experimental treatments within 18 months of capture.

Experimental protocol

Experiments were conducted using the IPOCAMP ∼19 litres (internal diameter 20 cm, internal depth 60 cm) stainless steel flow-through pressure system (Shillito et al., 2014). In brief, a seawater inlet line provides seawater (98.4±0.9%) from an 80 litre

Journal of Experimental Biology (2017) 220, 3916-3926 doi:10.1242/jeb.158543

reservoir to a high-pressure pump, which circulates seawater through the pressure vessel at a flow rate of 20 litres h^{-1}. A seawater outlet line is equipped with a manually operated back-pressure valve which controls pressure within the pressure circuit. Seawater pressurisation occurs within the circuit in the absence of gas bubbles; consequently, the partial pressure of dissolved gases remains unaltered at elevated pressure. Seawater is depressurised as it leaves the back-pressure valve, subsequently returning to the reservoir. Constant experimental temperature is achieved using a temperature regulation unit to circulate ethylene-glycol around the seawater inlet line and through steel jackets surrounding the pressure vessel. The system was run for 24 h prior to treatments to ensure the system was temperature acclimated and oxygen saturation was stable.

Experimental treatments were conducted following at least 2 months temperature acclimation to reduce potential impact of pre-capture temperature conditions. The reported distribution of *L. maja* is likely informed by adult occurrences, and sex and reproductive state may influence temperature and/or HP tolerance (George, 1984; Madeira et al., 2012). Consequently, mature males were used for all treatments. Maturity was assessed as >55 mm carapace length (CL), measured from the baseline of the orbit to the posterior edge of the carapace excluding protruding crests or spines (Macpherson, 1988; Snow, 2010). Maturity determination was based on the 0.87 male to female CL ratio for gonadal maturity established in the congeneric species *Lithodes santolla* (Vinuesa, 1984), and on personal observation (A.B.) of gonadal maturity through dissection or post-moult oviposition in 100% of female *L. maja* at ≤65 mm CL (n=5). CL was measured to the nearest 0.05 mm using vernier calipers. CL ranged from 56.0 to 102.5 mm. Total wet mass was determined to the nearest 0.1 g using an SG-5001 balance (Fisher Scientific). External body cavities (i.e. gill chambers) were drained by holding the animal perpendicular to the ground anterior downward for 1 min, and the animal was blotted dry. Total wet mass ranged from 231.5 to 841.7 g.

Five animals were exposed to control treatments and five to pressure treatments, and animals were not reused. Sample size power analysis was not performed because treatment effect sizes were entirely unknown. For each treatment, a single mature male was selected at random using numerical identifiers and random number generation. The investigator was not blinded to the treatment allocation. The animal was cleaned of encrusting detritus and epibiota to minimise potential for inaccuracies in oxygen consumption measurement, and starved for 7 days prior to experimental treatment to minimise potential for reduced HP tolerance resulting from specific dynamic action effects (Thatje and Robinson, 2011). Production of faecal matter ceased by 4 days post-feeding. A heartbeat sensor adapted for hyperbaric use (Robinson et al., 2009) was attached to the carapace over the cardiac region using dental wax and cyanoacrylate glue (Loctite, Henkel) and the animal was isolated in the IPOCAMP at 10:30 h. Twenty-four-hour darkness was maintained to simulate deep-sea light conditions and to minimise entrained light-dependent physiological cyclicity.

Acute hyperbaric tolerance

Stepped HP exposures were conducted at 6°C (salinity 32.7) across and beyond the range equivalent to the bathymetric distribution of *L. maja*. The experimental temperature was selected to match the temperature in the field at the time of sampling and to approximate the temperature of *L. maja*'s deepest recorded occurrence (6.6°C at 739 m depth) (OBIS, 2016). The experimental temperature also represented the deep-sea temperature at the proposed time of lithodid deep-sea radiation ∼15 million years ago (Hall and Thatje, 2009; Snow, 2010; Cramer et al., 2011; Bracken-Grissom et al., 2013) and is therefore within the thermal adaptive history of the genus, which may be key to understanding adaptive trajectories from shallow to deep living (New et al., 2014).

For control treatments, 0.1 MPa (≈surface pressure) was maintained for 240 h (Fig. 1). In pressure treatments, 0.1 MPa was maintained for 24 h then pressure was increased stepwise to 2.5 MPa (≈250 m depth) at 0.5 MPa 10 min^{-1}. Further stepwise 2.5 MPa increases were made at the same rate daily at 10:30 h, to a maximum pressure of 20.0 MPa. HP levels were selected to represent *L. maja*'s bathymetric distribution (0.1–7.5 MPa) and beyond (≥10.0 MPa). Subsequently, pressure was decreased to 0.1 MPa at 1.0 MPa 5 min^{-1}, and maintained to the end of the treatment (total treatment duration=240 h). Temperature and pressure within the system were recorded using a temperature/pressure logger (SP2T4000, NKE Instrumentation). Animals were removed, returned to maintenance conditions and observed daily for behavioural changes or mortality.

Sustained hyperbaric tolerance

Analysis of acute hyperbaric tolerance data indicated transition to moderate stress (*sensu* Sokolova, 2013) above 5.0 MPa and transition to extreme stress (*sensu* Sokolova, 2013) at 12.5 MPa (see below). Consequently, further hyperbaric tolerance exposures were conducted at 12.5, 10.0 and 7.5 MPa to assess sustained hyperbaric tolerance. The sustained hyperbaric tolerance protocol was a modification of the acute hyperbaric tolerance protocol to permit reuse of control treatment data (Fig. 2). As before, five animals were exposed to each treatment and animals were not reused. A pressure level of 0.1 MPa was maintained for 24 h, then pressure was increased stepwise to experimental pressure (12.5, 10.0 or 7.5 MPa) at 0.5 MPa 10 min^{-1}, and maintained to the end of the treatment (total treatment duration=240 h). Pressure was returned to 0.1 MPa over 1 min. Animals were removed and tissue was sampled for subsequent analysis of gene expression and phospholipid fatty acid composition; the third right pereopod was severed at the coxal end of the merus, and tissue was transferred to a 1.5 ml centrifuge tube and flash frozen in liquid nitrogen within 10 min of depressurisation. Acute depressurisation and rapid preservation were employed to minimise the potential for depressurisation artefacts and to minimise transcriptional recovery

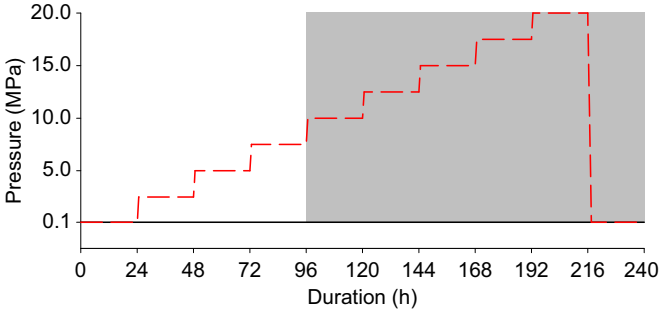

Fig. 1. Schematic representation of 240-h pressure treatments used to assess acute hyperbaric tolerance in adult male *Lithodes maja* at 6°C. Hydrostatic pressure was maintained at 0.1 MPa in the control treatment (black), whereas hydrostatic pressure was increased by 2.5 MPa at 24-h intervals in the hydrostatic pressure treatment (red). Incremental steps in pressure change are indicated as a straight line owing to scale. Shading indicates pressures greater than those within *L. maja*'s bathymetric distribution.

Journal of Experimental Biology (2017) 220, 3916-3926 doi:10.1242/jeb.158543

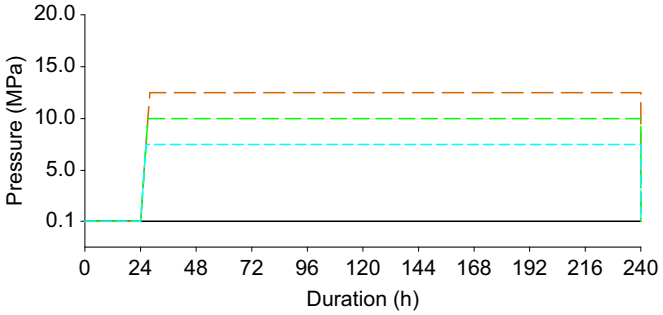

Fig. 2. Schematic representation of 240-h pressure treatments used to assess sustained hyperbaric tolerance in adult male *Lithodes maja* at 6°C. Hydrostatic pressure was maintained at 0.1 MPa in the control treatment (black), whereas hydrostatic pressure was increased after 24 h to 7.5 MPa (blue), 10.0 MPa (green) or 12.5 MPa (orange) in the hydrostatic pressure treatments. Incremental steps in pressure change are indicated as a straight line owing to scale.

(Morris et al., 2015c). Tissue was preserved at −80°C until analysed. Haemolymph was also sampled from 7.5 MPa-treated animals for L-lactate analysis; a sterile ice-cooled 23 g hypodermic needle (Neolus, Terumo) was inserted though the third left coxal arthroidal membrane and ∼0.5 ml haemolymph was withdrawn using a sterile 2 ml syringe (Plastipak, BD). Haemolymph samples were transferred to sterile 0.3 ml centrifuge vials and frozen at −20°C until analysed.

Heart rate and oxygen consumption data from the acute hyperbaric tolerance 0.1 MPa control treatment were available for direct comparison. However, tissue and haemolymph for sustained hyperbaric tolerance 0.1 MPa control treatments were sampled following the sustained hyperbaric tolerance protocol in an identical alternative IPOCAMP system. Although heart rate and oxygen consumption were not monitored in this sustained hyperbaric tolerance control treatment owing to limited equipment availability (i.e. only one Vernier LabPro system was available), a heartbeat sensor was attached to the carapace as previously described to minimise potential for treatment artefacts. Accurate temperature and HP calibration of the alternative system were confirmed using a temperature/pressure logger (SP2T4000, NKE Instrumentation).

Analysis of sustained hyperbaric tolerance heart rate and oxygen consumption data indicated a transient decrease in heart rate and sustained elevated oxygen consumption at 7.5 MPa (see below). Consequently, shorter duration hyperbaric exposures were conducted at 7.5 MPa to assess potential shifts in gene expression and haemolymph composition during sustained hyperbaric exposure. These hyperbaric acclimation treatments were conducted in the alternative system using a modification of the sustained hyperbaric tolerance protocol to permit comparison of tissue and haemolymph samples (Fig. 3). As before, five animals were exposed to each treatment and animals were not reused. A heartbeat sensor was attached to the carapace despite no heart rate or oxygen consumption data being recorded, to minimise potential for treatment artefacts. A pressure level of 0.1 MPa was maintained for 24 h, then pressure was maintained at 0.1 MPa for 6 h 20 min or 26 h 20 min (control treatments), or increased stepwise to experimental pressure (7.5 MPa) at 0.5 MPa 10 min^{-1} and maintained for 4 or 24 h, achieving consistent sampling time and eliminating potential confounding from diel cyclic variability. Treatments were terminated and tissue and haemolymph were sampled following the sustained hyperbaric tolerance protocol.

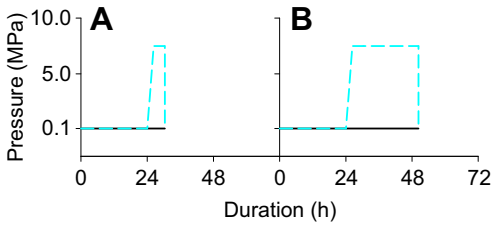

Fig. 3. Schematic representation of pressure treatments used to assess hyperbaric acclimation in adult male *Lithodes maja* at 6°C. (A) 4 h treatment; (B) 24 h treatment. Hydrostatic pressure was maintained at 0.1 MPa in the control treatment (black), whereas hydrostatic pressure was increased after 24 h to 7.5 MPa (blue) in the hydrostatic pressure treatments. Incremental steps in pressure change are indicated as a straight line due to scale.

Physiological measurements

Measuring heart rate and oxygen consumption

Heart rate (beats min^{-1}) was assessed through movements of the cardiac muscle, recorded using the photoplethysmographic technique, which is as precise and accurate as the impedance method but is non-invasive (Burnett et al., 2013). The photoplethysmographic sensor emits infrared light, which penetrates the carapace and is backscattered by the underlying heart tissue. The direction and intensity of the backscatter depend on the shape of the tissue. Any change in backscatter reflects the contraction and relaxation of the cardiac muscle and is detected by the sensor. Raw signal was recorded at a sampling rate of 1000 min^{-1}, converted into voltage and transmitted to a voltage amplifier (Electrode Amplifier, Vernier), before the analogue signal was digitalised by the LabPro system (Vernier), and recorded and interpreted using LoggerPro software (version 3.4.2, Vernier).

Mass-specific molar oxygen consumption (O_C, μmol g^{-1} h^{-1}) was calculated from the decrease in oxygen concentration between inflow seawater (O_I, % saturation) and outflow seawater (O_O, % saturation) using the equation:

$$O_C = (((O_I - O_O)/100) \times O_S \times F)/M, \quad (1)$$

where O_S is the molar oxygen concentration of oxygen-saturated seawater (μmol l^{-1}) calculated according to Benson and Krause (1984), F is the seawater flow rate (20 litres h^{-1}) and M is total wet mass (g). Oxygen saturation of seawater was measured and recorded using an oxygen microoptode connected to a Microx TX3 array (PreSens) at a sampling rate of 1 Hz (Thatje and Robinson, 2011).

Heart rate and oxygen consumption were recorded over the duration of the treatment, but the large quantity of data collected made it necessary to interrupt recording briefly (<10 min for heart rate; <1 min for oxygen consumption) every 12 h (09:00 and 21:00 h) to store data and reset software. Oxygen saturation did not fall below 75% (=236.9 μmol O_2 l^{-1}) during any treatment, reducing the potential for hypoxic exposure effects (McMahon, 2001; Vaquer-Sunyer and Duarte, 2008; Brown and Thatje, 2015).

Heart rate and oxygen consumption data normalisation and statistical analysis

Mean mass of individuals used in each experimental treatment (n=5) did not vary significantly (one-way ANOVA, $F_{4,20}$=0.668, P=0.622; data were normally distributed and homoscedastic: Shapiro–Wilk test, P=0.994; Levene's test, P=0.141). Means were calculated for heart rate and mass-specific molar oxygen consumption for each 1 h period of the treatment. Data were subsequently normalised to the mean mass of experimental subjects (464.5 g) to compensate for significant mass-dependent variation in

heart rate and mass-specific molar oxygen consumption (non-linear regression using a power function: $F_{2,23}$=4.362, P=0.048 and $F_{1,23}$=9.676, P=0.005, respectively). Mass-scaling functions were derived using data from all specimens (control and experimental, acute and sustained hyperbaric tolerance) at 0.1 MPa over the initial 24 h of treatments (n=25), assuming intraspecific mass scaling follows a power function (Glazier, 2005). Both heart rate and mass-specific molar oxygen consumption mass-scaling exponents (−0.232 and −0.595, respectively) were within the range reported elsewhere (Glazier, 2005; West and Brown, 2005). Linear regression of mass-normalised heart rate (f_H) and mass-normalised mass-specific molar oxygen consumption ($\dot{M}_{O_2}$, µmol g^{-1} h^{-1}) indicated mass independence ($F_{1,23}$=0.000, P=0.998 and $F_{1,23}$=0.078, P=0.783, respectively).

Daily rhythms were evident in f_H and $\dot{M}_{O_2}$ in control treatments, limiting comparisons between treatments to corresponding periods. To integrate diel variation into the statistical analysis, means were calculated for the period at which all treatments were at experimental pressure, i.e. the last 22 h of each 24-h period for acute hyperbaric tolerance treatments, and the last 18 h of each 24-h period for sustained hyperbaric tolerance treatments. f_H means for acute hyperbaric tolerance and sustained hyperbaric tolerance were homoscedastic (Levene's test, P=0.952 and P=0.316). $\dot{M}_{O_2}$ means for acute hyperbaric tolerance and sustained hyperbaric tolerance were square-root transformed to achieve homoscedasticity (Levene's test, P=0.116 and P=0.639). The effect of HP on f_H and $\dot{M}_{O_2}$ was assessed using two-way repeated measures ANOVA, with treatment (control or HP) and exposure duration (proxy for HP in pressure treatments) as fixed factors (α=0.05). The *post hoc* Holm–Sidak multiple comparisons test was used to determine significant differences from the initial 0.1 MPa period within both control and pressure treatments, and significant differences between control and pressure treatments during corresponding periods.

Gene expression

Endogenous reference genes and genes of interest were identified from the literature. Two reference genes (*eef1a* and *rpl8*) were tested based on previous use in assessing transcriptional responses in *L. maja* (8): *eef1a* codes for eukaryotic translation elongation factor 1 alpha and *rpl8* codes for ribosomal protein L8.

Centrifuge tubes (1.5 ml) containing individual tissue samples were removed from −80°C storage and immersed in liquid nitrogen. Tissue samples were immediately transferred into 2 ml of TRI Reagent (Sigma-Aldrich) and homogenised using an Ultra Turrax (Ika). The manufacturer's standard protocol was followed during total RNA extraction. A Nanodrop spectrophotometer (Thermo Fisher Scientific) was used to test total RNA purity. All samples recorded a 260 nm/280 nm ratio above 1.8, and a 260 nm/230 nm ratio above 1.9. Experion (Bio-Rad) was used to evaluate total RNA integrity and concentration: all samples recorded an RQI (RNA quality indicator) above 8.5 and concentration above 300 ng $µl^{-1}$. RQ1 RNase-free DNase (Promega) was used according to the manufacturer's protocol to DNase treat a volume containing 1.5 µg of total RNA. Superscript IIITM (Invitrogen) and oligo (dT)18–23 primers were used according to the manufacturer's protocol to reverse transcribe 0.75 µg total RNA in a 20 µl reaction.

Primer sequence data for quantitative polymerase chain reaction (qPCR) were obtained from Munro et al. (2015). Reaction amplification was optimised by testing each qPCR assay at a variety of mixed primer concentrations. Melt curve analysis generated a single and discrete peak for all primer sets tested. Following determination of optimal concentrations for both forward and reverse primers (Munro et al., 2015), qPCR reaction efficiency between 90 and 105% and linearity greater than r^2=0.98 were confirmed for each primer set across the predicted experimental cDNA concentration range by 10-fold serial dilutions performed on a cDNA template, as set out by the MIQE guidelines (Bustin et al., 2009).

The Rotor-Gene 3000 (Qiagen) was used for all qPCR reactions. Each 25 µl reaction contained 12.5 µl of Precision 2× qPCR Master mix with SYBR Green (Primer-Design, UK), and 2 µl of template cDNA (34 ng). qPCR conditions were: one cycle of 95°C for 10 min followed by 40 cycles of 95°C for 10 s and 60°C for 1 min. Each reaction was duplicated for technical replication. Specificity of the qPCR products was demonstrated by melt curve analysis after each run.

Relative stability of reference gene expression across experimental treatments was analysed using the geNorm function within qBase+ software (Biogazelle). The best normalisation strategy was delivered by the combination of *eef1a* and *rpl8*. qBase+ was used to calculate normalised relative quantities. Statistically significant differences were assessed within each exposure duration treatment by one-way ANOVA (α=0.05). The *post hoc* Tukey–Kramer test within qBase+ software was used to determine which treatments differed significantly from the corresponding control treatment.

Phospholipid fatty acid composition

Centrifuge tubes (1.5 ml) containing individual tissue samples were removed from −80°C storage and individual tissue samples were homogenised (using an IKA T10 Basic Ultra-Turrax homogenizer) in chloroform:methanol (2:1, v/v) and total lipid was extracted according to Folch et al. (1957). Following the addition of aqueous potassium chloride (0.88%, w/v), samples were thoroughly vortexed, then centrifuged for 5 min at 400 ***g*** to establish a biphasic system. The upper phase (aqueous methanol layer containing non-lipid substances) was removed via pipetting, and discarded. The lower phase (chloroform layer containing lipid) was filtered through pre-washed (with chloroform:methanol 2:1, v/v) Whatman no. 1 filter paper into pre-weighed vials. Samples were then dried down under N_2 gas (using an N-EVAP system, Organomation), placed in a desiccator for 1 h, weighed to establish total lipid mass, and redissolved in chloroform (1 mg ml^{-1} final concentration). Samples were then stored at −20°C.

Phospholipids were purified by thin layer chromatography (TLC); a 1 mg aliquot of total lipid was run on 2 mm, 20×20 cm silica gel plates in a hexane:diethyl ether:acetic acid (80:20:2, v/v/v) solvent system. Plates were sprayed with 2′,7′dichloro-fluorescein in methanol (0.1%, w/v) to enable lipid visualisation under ultraviolet light. Phospholipids were scraped off plates into vials in which trans-methylation reactions were established (following Christie, 1982) by dissolving scrapings in 1% sulphuric acid in methanol and toluene (1:2, v/v) and incubating at 50°C for 16 h. Post-trans-methylation, equal volumes of deionised milli-Q water and hexane:diethyl ether (1:1, v/v) were added and samples were mixed thoroughly via vortexing. Centrifuging (for 2 min at 400 ***g***) established a biphasic system, the upper phase of which was removed into a vial. Aqueous sodium bicarbonate (2%, w/v) was added and samples were mixed thoroughly via vortexing, and centrifuged (for 2 min at 400 ***g***) to establish a biphasic system, of which the upper solvent fraction was removed into vials and dried down under N_2 gas. This purified phospholipid fraction was redissolved in ∼0.1 ml hexane and run through a TRACE2000 Thermo Electron Gas Chromatograph (Thermo Scientific, UK)

Journal of Experimental Biology

Journal of Experimental Biology (2017) 220, 3916-3926 doi:10.1242/jeb.158543

equipped with a Restek Stabilwax column (0.32 mm internal diameter ×30 m) with hydrogen used as the carrier gas (Pond et al., 2014).

Phospholipid fatty acid composition data were proportional and were therefore arcsine-square-root transformed prior to statistical analysis. Statistically significant differences within each exposure duration treatment were assessed by one-way ANOVA, with HP as the fixed factor (α=0.05).

Haemolymph lactate concentration

Haemolymph subsamples (10 µl) were deproteinised by addition of 10 µl 0.6 mol l^{-1} perchloric acid. Subsamples were subsequently neutralised by addition of 2.5 mol l^{-1} potassium carbonate. The denatured sample was centrifuged at 10,000 ***g*** for 20 min at 4°C and the supernatant was removed for use in the L-lactate assay. Haemolymph L-lactate concentration was determined in a microplate reader (FLUOstar OPTIMA, BMG Labtech) at 552 nm absorbance using a lactate assay kit (Trinity Biotech).

L-lactate concentrations were normal and homoscedastic (Shapiro–Wilk test, P>0.05; Levene's test, P>0.05). Statistically significant differences within each exposure duration treatment were assessed by one-way ANOVA, with HP as the fixed factor (α=0.05).

RESULTS

Survival

All individuals (n=10) survived the duration of the acute hyperbaric tolerance exposures (Fig. 1) and survived ≥3 months post-treatment. Individuals exposed to the control treatment (n=5) resumed normal behaviour (e.g. feeding) immediately upon return to the aquarium. In contrast, individuals exposed to the pressure treatment (n=5) were quiescent for several days following treatment before resuming normal activity. Individuals from both treatments later moulted and engaged in mating. All individuals (n=25) also survived the duration of the sustained hyperbaric tolerance treatments (Fig. 2), but post-treatment survival following tissue sampling varied: all individuals exposed to 0.1 MPa control and 7.5 MPa pressure treatments (n=10) survived; three individuals exposed to the 10.0 MPa pressure treatment (n=5) survived; no individuals exposed to the 12.5 MPa pressure treatment (n=5) survived. Differences in post-treatment survival following tissue sampling may reflect differences in the extent of impacts resulting from acute depressurisation from 7.5, 10.0 and 12.5 MPa. All individuals (n=20) survived the duration of the hyperbaric acclimation treatments (Fig. 3) as well, and survival following tissue sampling again varied: all individuals exposed to 4-h and 24-h 0.1 MPa treatments (n=10) survived; no individuals exposed to 4-h and 24-h 7.5 MPa treatments (n=10) survived.

Acute hyperbaric tolerance

The effect of exposure duration (a proxy for HP in pressure treatments) on mean f_H and mean $\dot{M}_{O_2}$ depended on treatment (respectively, $F_{9,72}$=9.374, P<0.001 and $F_{9,72}$=5.669, P<0.001; Fig. 4). Mean f_H and $\dot{M}_{O_2}$ remained approximately constant in the control treatment. In contrast, mean f_H and $\dot{M}_{O_2}$ differed among periods in the pressure treatment.

Mean f_H in the pressure treatment was significantly lower at pressures ≥10.0 MPa than during corresponding periods in the control treatment; mean f_H decreased with each pressure increase. Rhythms evident in control treatment f_H appeared reduced in the pressure treatment at 5.0 and 7.5 MPa relative to corresponding periods in the control treatment, and were not apparent at pressures ≥10.0 MPa. Variability in f_H appeared reduced at pressures of ≥12.5 MPa. Rhythms did not recommence after depressurisation to 0.1 MPa. f_H increased rapidly after depressurisation and continued to increase over time; mean f_H was significantly greater than during the corresponding period in the control treatment.

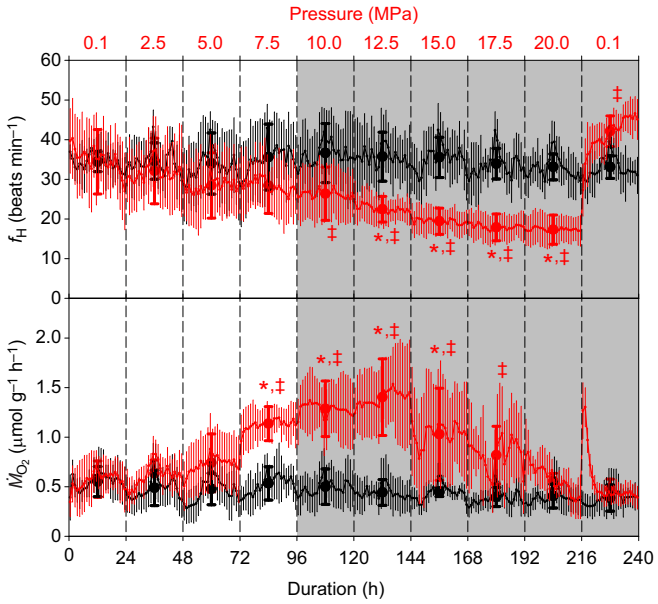

Fig. 4. Effect of hydrostatic pressure on heart rate (f_H) and molar oxygen consumption ($\dot{M}_{O_2}$) in adult male *Lithodes maja* at 6°C. Hydrostatic pressure was maintained at 0.1 MPa in the control treatment (black), whereas hydrostatic pressure was increased by 2.5 MPa at 24-h intervals in the hydrostatic pressure treatment (red; n=5 individuals; see Fig. 1). Continuous data are presented as mean values for each hour. Filled circles present mean values for each 24-h period, which were used in statistical analysis (two-way repeated-measures ANOVA with *post hoc* Holm–Sidak multiple comparisons test; α=0.05). Error bars represent 95% confidence intervals. Significant differences from the initial 24-h period within a treatment are indicated by asterisks; significant differences between control and pressure treatments within a time period are indicated by double daggers; colour reflects treatment. Shading indicates pressures greater than those within *L. maja*'s bathymetric distribution.

Mean $\dot{M}_{O_2}$ in the pressure treatment was significantly greater at pressures of 7.5 to 17.5 MPa than during corresponding periods in the control treatment; mean $\dot{M}_{O_2}$ increased with each pressure increase to 12.5 MPa, before decreasing with each pressure increase to 20.0 MPa. Rhythms evident in control treatment $\dot{M}_{O_2}$ appeared reduced in the pressure treatment at 5.0 MPa, and were not apparent at pressures ≥7.5 MPa. At 17.5 MPa $\dot{M}_{O_2}$ appeared to decline initially before rising again, and at 20.0 MPa $\dot{M}_{O_2}$ appeared to decline over time. Rhythms did not recommence after depressurisation to 0.1 MPa. $\dot{M}_{O_2}$ rose rapidly after decompression but declined over time; mean $\dot{M}_{O_2}$ was not significantly different from the corresponding period in the control treatment.

Sustained hyperbaric tolerance

The effect of exposure duration on mean f_H and mean $\dot{M}_{O_2}$ depended on treatment (respectively, $F_{27,144}$=3.557, P<0.001 and $F_{27,144}$=4.647, P<0.001; Fig. 5). In the control treatment, mean f_H and mean $\dot{M}_{O_2}$ remained approximately constant. In contrast, mean f_H demonstrated a sustained significant decrease at 12.5 MPa, and a transient significant decrease at 10.0 and 7.5 MPa. Mean $\dot{M}_{O_2}$ demonstrated a sustained significant increase in all pressure treatments.

Journal of Experimental Biology (2017) 220, 3916-3926 doi:10.1242/jeb.158543

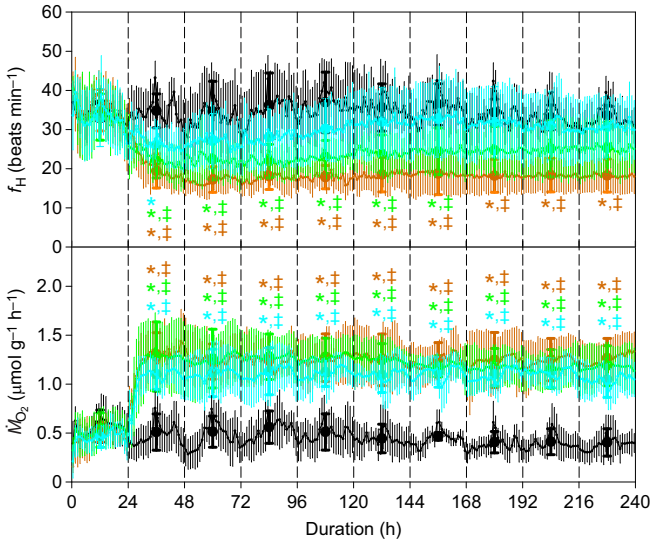

Fig. 5. Effect of sustained hydrostatic pressure on heart rate (f_H) and molar oxygen consumption ($\dot{M}_{O_2}$) in adult male *Lithodes maja* at 6°C. Hydrostatic pressure was maintained at 0.1 MPa in the control treatment (black), whereas hydrostatic pressure was increased after 24 h to 7.5 MPa (blue), 10.0 MPa (green) or 12.5 MPa (orange) in the hydrostatic pressure treatments (n=5 individuals; see Fig. 2). Continuous data are presented as mean values for each hour. Filled circles present mean values for each 24-h period, which were used in statistical analysis (two-way repeated-measures ANOVA with *post hoc* Holm–Sidak multiple comparisons test; α=0.05). Error bars represent 95% confidence intervals. Significant differences from the initial 24-h period within a treatment are indicated by asterisks; significant differences between control and pressure treatments within a time period are indicated by double daggers; colour reflects treatment.

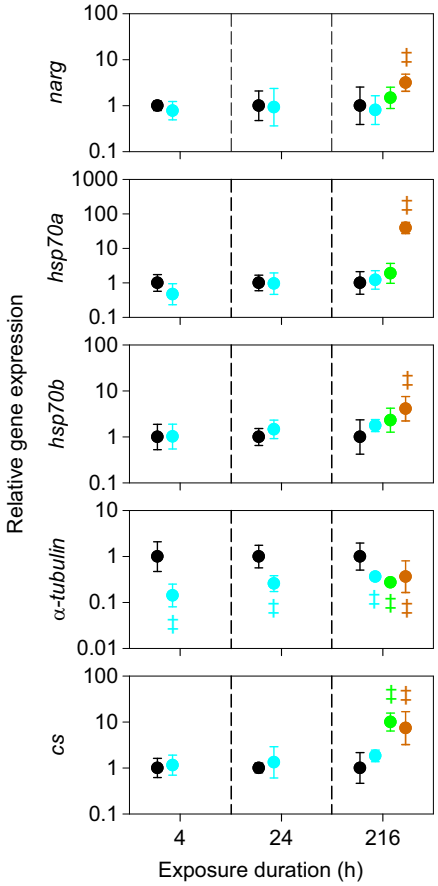

Fig. 6. Effect of hydrostatic pressure on gene expression in adult male *Lithodes maja* at 6°C. Hydrostatic pressure was maintained at 0.1 MPa in the control treatment (black), whereas hydrostatic pressure was increased to 7.5 MPa (blue), 10.0 MPa (green) or 12.5 MPa (orange) in the hydrostatic pressure treatments (n=5 individuals; see Figs 2 and 3). Data present expression relative to expression at 0.1 MPa; data points are offset for clarity. Error bars represent 95% confidence intervals. Significant differences between control and pressure treatments within a time period are indicated by double daggers (one-way ANOVA with *post hoc* Holm–Sidak multiple comparisons test; α=0.05); colour reflects treatment.

Gene expression

Expression of *narg*, *hsp70a*, *hsp70b* and *cs* were not significantly affected by exposure to 7.5 MPa after any exposure duration (P>0.05; Fig. 6). However, *narg*, *hsp70a*, *hsp70b* and *cs* expression were significantly upregulated after 216 h at 12.5 MPa (P<0.05), and *cs* was also significantly upregulated after 216 h at 10.0 MPa (P<0.05). In contrast, *α-tubulin* expression was significantly downregulated at elevated pressure after all exposure durations (P<0.05).

Phospholipid fatty acid composition

Phospholipid fatty acid composition was not significantly affected by HP after any treatment duration (P>0.05) (Fig. 7).

Haemolymph lactate concentration

Haemolymph lactate concentration was not significantly affected by HP after any treatment duration (P>0.05) (Fig. 8).

DISCUSSION

The metabolic rate of *L. maja* increased significantly between 5.0 and 12.5 MPa (equivalent to approximately 1250 m depth) (Figs 4 and 5). Pressure effects on biochemical reaction rates (Picard and Daniel, 2013) may contribute to the exponential increase in mean metabolic rate in *L. maja* between 0.1 and 12.5 MPa ($F_{1,4}$=74.45, P=0.001; r^2=0.949). For example, increasing TCA cycle enzyme activities with increasing pressure (Gerringer et al., 2017) may drive hyperbaric increases in metabolic rate. Pressure-sensitive metabolic rate suggests a role for HP within both the metabolic theory of ecology (Brown et al., 2004) and the metabolic framework for ecology and evolution (Sibly et al., 2012), which focus on ecological effects on metabolic rate and consequent impacts on ecological and evolutionary processes. Hyperbaric effects on metabolic rate mediated through reaction kinetics and energy demand may influence macroecological patterns of decreasing abundance and biomass with depth, the species–energy framework structuring oceanic biodiversity, and deep-sea ecosystem functioning, by accentuating the effects of bathymetric decrease in chemical energy availability (Brown and Thatje, 2014; Jones et al., 2014; Woolley et al., 2016). Similarly, hyperbaric effects on metabolic rate may influence bathymetric diversity patterns by increasing metabolic-rate-dependent mutation in shallow-water taxa invading the deep sea (Brown and Thatje, 2014). However, hyperbaric increases in metabolic rate probably also reflect responses to moderate stress (*sensu* Sokolova, 2013) imposed by hydrostatic pressure: cellular, physiological and/or behavioural responses impose substantial energetic costs (Sokolova, 2013).

The decrease in metabolic rate at HP greater than 12.5 MPa (Fig. 4) likely represents a distinct physiological response indicating extreme stress (*sensu* Sokolova, 2013). Decreasing metabolic rate at HP greater than 12.5 MPa is unlikely to result from a hyperbaric kinetic bottleneck in respiratory exchange rate: pressure decreases the oxygen concentration required to support a given uptake rate

Journal of Experimental Biology (2017) 220, 3916-3926 doi:10.1242/jeb.158543

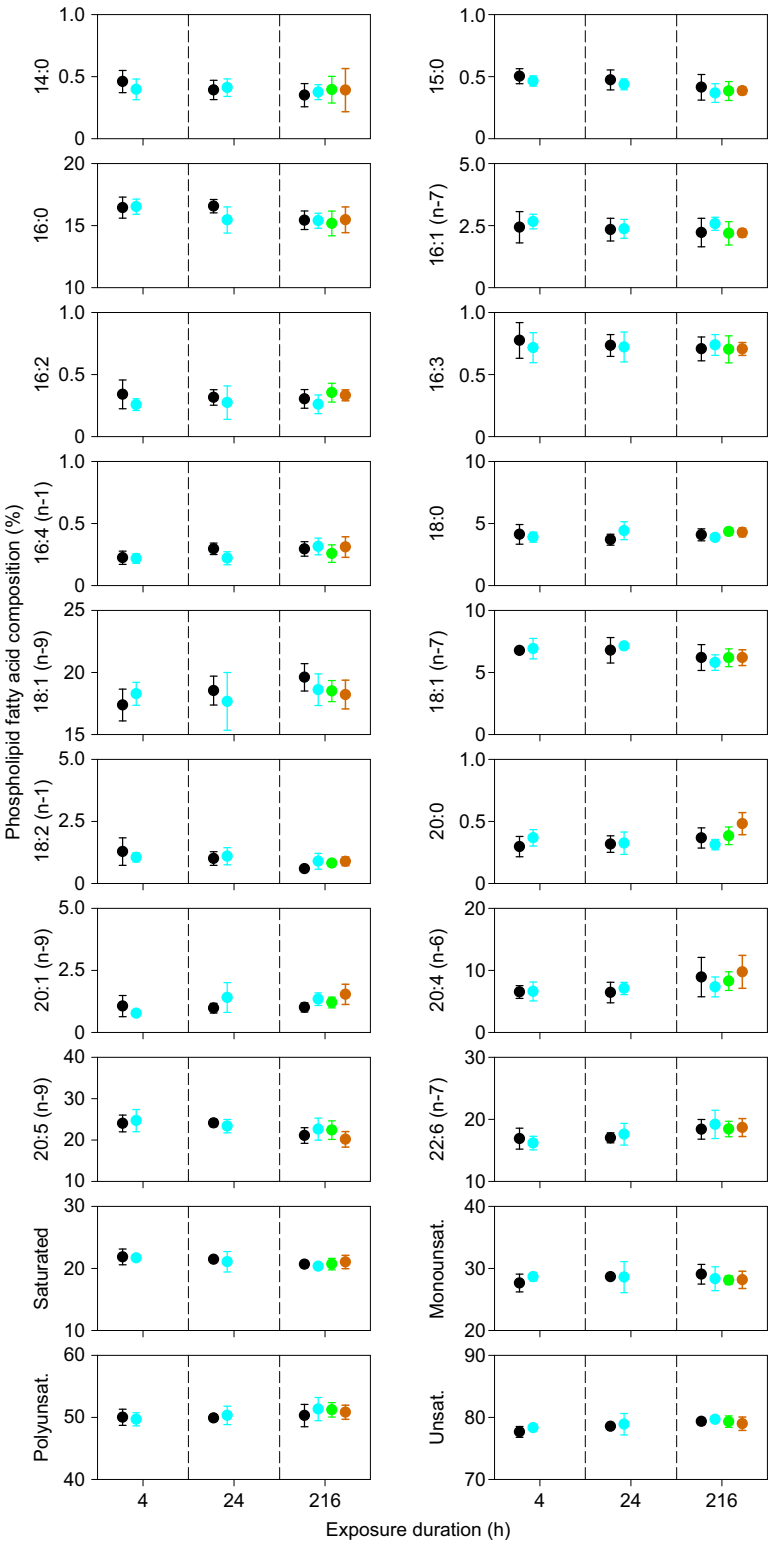

Fig. 7. Effects of hydrostatic pressure on phospholipid fatty acid composition in adult male *Lithodes maja* at 6°C. Hydrostatic pressure was maintained at 0.1 MPa in the control treatment (black), whereas hydrostatic pressure was increased to 7.5 MPa (blue), 10.0 MPa (green) or 12.5 MPa (orange) in the hydrostatic pressure treatments (n=5 individuals; see Figs 2 and 3). Data points are offset for clarity. Error bars represent 95% confidence intervals. There were no significant differences between control and pressure treatments within a time period (one-way ANOVA; α=0.05).

(Hofmann et al., 2013b), the key limiting chemical exchange rate (Hofmann et al., 2013a). Instead, significant increases in metabolic rate may result in elevated internal P_{CO_2} (Fehsenfeld and Weihrauch, 2017). Acid–base homeostasis mechanisms may be insufficient at high hydrostatic pressure or may be disrupted by hyperbaric effects on cell membrane function (Brown and Thatje, 2014), leading to metabolic and respiratory acidosis and, consequently, to impairment of aerobic metabolism (Fehsenfeld and Weihrauch, 2017). Progressive impairment of aerobic metabolism during high stress typically results in a slowing of metabolic activity and suppression of metabolic rate (Sokolova, 2013). Elevated metabolic rate and heart rate in *L. maja* following return to 0.1 MPa (surface pressure) is consistent with this interpretation, suggesting restitution for an oxygen debt and/or readjustment of acid–base status. A similar response is observed following alleviation of extreme hypoxic stress (Hill et al., 1991).

Journal of Experimental Biology (2017) 220, 3916-3926 doi:10.1242/jeb.158543

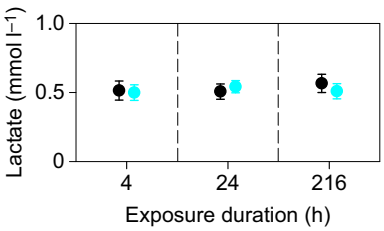

Fig. 8. Effects of hydrostatic pressure on haemolymph lactate concentration in adult male *Lithodes maja* at 6°C. Hydrostatic pressure was maintained at 0.1 MPa in the control treatment (black), whereas hydrostatic pressure was increased to 7.5 MPa (blue) in the hydrostatic pressure treatments (n=5 individuals; see Figs 2 and 3). Data points are offset for clarity. Error bars represent 95% confidence intervals. There were no significant differences between control and pressure treatments within a time period (one-way ANOVA; α=0.05).

In contrast to metabolic rate, heart rate decreased progressively between 7.5 and 20.0 MPa (Figs 4 and 5). The patterns in metabolic rate and heart rate response to HP are strikingly similar to patterns in metabolic rate and heart rate reported in response to decreasing oxygen concentration and progressive hypoxia (e.g. Wheatly and Taylor, 1981), suggesting that hyperbaric tolerance in *L. maja* may be oxygen limited. The hyperbaric tolerance of other bathyal crustaceans appears similarly limited. Heart rate decreases in the deep-sea hydrothermal vent crab *Bythograea thermydron* at pressures above and below the species' bathymetric distribution, with concomitant increases in oxygen consumption (Mickel and Childress, 1982a,b; Airriess and Childress, 1994). Indeed, as HP increases beyond native pressure, heart rate decreases by 0.85 beats min^{-1} MPa^{-1} in *B. thermydron* (Airriess and Childress, 1994), strikingly similar to the 0.89 beats min^{-1} MPa^{-1} hyperbaric heart rate decrease in *L. maja* (Figs 4 and 5). Consistent heart rate responses in these species suggest that a common mechanism may determine heart rate responses to elevated HP in crustaceans.

Hyperbaric exposure depresses synaptic transmission, including in the neuromuscular junction of shallow-water crustaceans at 5.0 MPa (Campenot, 1975), interfering with neurogenic muscle regulation and mediating decreases in heart rate (Sébert, 2010). NMDA receptors are present in the central nervous system in all eumetazoans (Ryan and Grant, 2009), and are concentrated in major ganglia of decapods, demonstrating strong localisation in synaptosomal membranes (Hepp et al., 2013). HP diminishes the efficacy of NMDA receptor blockade and modulates NMDA receptor ionic currents, leading to synaptic delay (Mor and Grossman, 2010). Transcription of *narg* codes for an NMDA receptor-regulated protein and has been identified as a hyperbaric neurophysiological stress marker (Morris et al., 2015a,b,c; Munro et al., 2015). The NMDA receptor response (inferred from differential *narg* transcription) reflects whole-organism hyperbaric performance (Morris et al., 2015a,b,c; Munro et al., 2015). Decreasing heart rate in *L. maja* therefore probably results from depressed neurotransmission. Upregulation of *narg* transcription in *L. maja* at 12.5 MPa reflects shifts in NMDA receptor activity, with the concomitant upregulation of *hsp70* indicating stimulation of the ubiquitous cellular stress response to significant macromolecular damage (Fig. 6) (Morris et al., 2015a,b,c; Munro et al., 2015). Elevated internal P_{CO_2} may also contribute to decreasing heart rate (Ashby and Larimer, 1964) mediated by metabolic and respiratory acidosis: significant increases in metabolic rate may result in elevated internal P_{CO_2} (Fehsenfeld and Weihrauch, 2017) and/or acid–base homeostasis mechanisms may be disrupted by hyperbaric effects on ion transporters (Brown and Thatje, 2014). Acidosis may be assessed in future experiments by measuring acid–base parameters and/or activities of enzymes involved in acid–base regulation, or by assessing transcription of genes involved in acid-base homeostasis. Recovery in heart rate following transient decreases at 7.5 and 10.0 MPa indicates hyperbaric acclimation, compensating for acute synaptic effects of high HP and/or internal P_{CO_2} effects (Fig. 5). Heart rate acclimation in *L. maja* is not mediated by shifts in membrane phospholipid fatty acid composition (Fig. 7), suggesting mediation by ion transporters or ion channels such as NMDA receptors instead.

In contrast, the shift in *narg* transcription at 12.5 MPa endures (Fig. 6), and interference with neurogenic heart rate persists. Putative pressure adaptations make excitatory synaptic potential in the deep-sea brachyuran crab *Chaceon quinquidens* insensitive to HP up to at least 20.0 MPa (Campenot, 1975), indicating that adaptation in cell surface receptors may be key to deep-sea colonisation; the bathymetric range of *C. quinquidens* extends to 2285 m water depth (OBIS, 2016). The fundamental importance of synaptic function implies that this mechanism will limit hyperbaric tolerance in eumetazoans (Ryan and Grant, 2009), although variation in dependence on heart rate may modulate critical hyperbaric thresholds (Brown and Thatje, 2015). Elucidating these mechanisms constraining hyperbaric tolerance may be crucial to understanding the evolution of the extant deep-sea fauna and adaptation of life at depth: deep continental margins are putatively the principal site of adaptive radiation and speciation in the deep sea (Brown and Thatje, 2014). However, recovery in heart rate at HP equivalent to approximately 1000 m depth (10.0 MPa) indicates that it is not the critical hyperbaric threshold that defines the limit to *L. maja*'s 4–790 m bathymetric range. Is there another mechanism through which HP may limit biogeographic range?

Species' biogeographic range limits typically occur before the transition to extreme stress (Pörtner and Farrell, 2008; Sokolova, 2013). For example, environmental temperatures in marginal populations of many aquatic ectotherms correlate with the critical temperatures at which these organisms transition to moderate stress, and therefore thermal boundaries of species distributions appear determined by the energetic costs involved in moderate stress responses (Pörtner and Farrell, 2008; Sokolova, 2013). These responses may be mediated by cellular, physiological and/or behavioural mechanisms, such as those involved in maintaining acid–base homeostasis (Fehsenfeld and Weihrauch, 2017), requiring flexible energy resource allocation and/or metabolic power (Sokolova, 2013). In the dynamic energy budget model, energy assimilated by an organism is divided among maintenance, activity, development/growth and reproduction (Kooijman, 2010). Maintenance costs comprise energy demands for basal cellular and organismal maintenance supporting key cellular processes (e.g. ion regulation, protein turnover) and essential systemic activities such as ventilation and circulation. Somatic maintenance is the dominant energy budget component and cannot be reduced below a fundamental level. Surplus energy may be deposited as an energy reserve and the reserve rapidly provides energy to meet any elevated metabolic cost of maintenance during moderate stress. However, individual fitness is reduced by moderate stress as additional homeostatic energy costs lead to energetic trade-offs and result in reduced activity, scope for growth, and/or reproductive output (Sokolova, 2013). For example, increased allocation of energy to maintenance diminishes energy available for other functions such as buffering fluctuating food availability or provisioning offspring (Sokolova, 2013).

Moderate stress typically induces a transition from a state of cellular growth to one of cellular maintenance (Kassahn et al.,

Journal of Experimental Biology (2017) 220, 3916-3926 doi:10.1242/jeb.158543

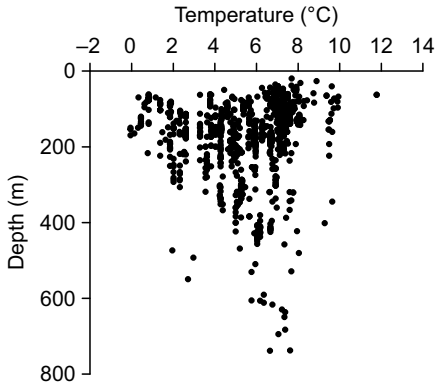

Fig. 9. Thermal and bathymetric distribution of *Lithodes maja*. Data are from OBIS (2016) and represent single records.

2009), which is reflected in sustained downregulation of *α-tubulin* at 7.5–12.5 MPa in *L. maja* (Fig. 6). Microtubule tubulin polymers are essential cytoskeletal components affecting cell division in all eukaryotes, and downregulation of *α-tubulin* will reduce microtubule filament formation, with a multiplicity of cascading cellular effects (Nogales, 2000). At the whole-organism level, compensatory mechanisms involve accelerated oxygen uptake to support increasing allocation of energy to maintenance (Willmer et al., 2005). Increasing allocation of energy to maintenance is evident in elevated and increasing oxygen consumption at 7.5–12.5 MPa in *L. maja* (Figs 4 and 5), and is also apparent in upregulated *cs* expression (Fig. 6). Expression of the *cs* gene is correlated with mitochondrial citrate synthase activity, a key and rate-limiting constituent of the TCA cycle (Stager et al., 2015). Moderate stress reflected in elevated metabolic rate and in transcriptional responses is sustained at 7.5–12.5 MPa despite acclimation in f_H at 7.5 and 10.0 MPa (Figs 5 and 6), without increased dependence on anaerobic respiration, at least at 7.5 MPa (Fig. 8). The transition to sustained moderate hyperbaric stress in *L. maja* precedes the 790 m bathymetric limit to the species' known distribution (Fig. 9), and it is therefore evident that it is the metabolic cost associated with moderate hyperbaric stress, reflected in sustained elevated metabolic rate, that constrains *L. maja*'s bathymetric distribution. This interpretation advocates incorporating HP in a matrix of energy-limited biogeographic range in marine ectotherms, dependent on the energetic costs associated with tolerance of interacting suboptimal environmental conditions including temperature, dissolved oxygen concentration and dissolved carbon dioxide concentration (Sokolova, 2013). Recognising the role of HP in constraining the biogeographic range of marine ectotherms is thus essential to evaluating accurately the effects of climatic change on species' depth distributions, which may be of equal importance to effects on latitudinal distributions (Brown and Thatje, 2015; Morris et al., 2015a).

Acknowledgements

Results in this paper are reproduced from the PhD thesis of Alastair Brown (University of Southampton, 2015). The authors are grateful to Bengt Lundve (organised sampling of crabs and maintenance prior to transportation), Tony Roysson (led the fieldwork), Adam J. Reed (provided detailed advice on aquarium construction for long-term maintenance of crabs) and Neil Jenkinson (constructed the heartbeat sensors). The authors thank Bruce Shillito for complementary discussions. The authors thank an anonymous reviewer for constructively discussing this article.

Competing interests

The authors declare no competing or financial interests.

Author contributions

Conceptualization: A.B., S.T.; Methodology: A.B., S.T., J.P.M., A.O., E.A.M., C.H.; Formal analysis: A.B., J.P.M., A.O., E.A.M.; Investigation: A.B., J.P.M., A.O., E.A.M.; Resources: A.B., S.T., C.H., D.O.B.J., D.W.P.; Data curation: A.B.; Writing - original draft: A.B.; Writing - review & editing: A.B., S.T., J.P.M., A.O., E.A.M., C.H., D.O.B.J., D.W.P.; Visualization: A.B.; Supervision: A.B., S.T., C.H., D.O.B.J., D.W.P.; Project administration: A.B.; Funding acquisition: A.B., S.T., C.H., D.O.B.J., D.W.P.

Funding

A.B. was supported through a Natural Environment Research Council (NERC) PhD studentship and a Collaborative Award in Science and Engineering from Transocean. J.P.M. was supported through a NERC PhD studentship. A.O. was supported through a Marine Alliance for Science and Technology for Scotland bursary to D.W.P. and S.T. D.O.B.J. was supported through NERC National Capability funding to the National Oceanography Centre. This study was supported by grants from ASSEMBLE (Seventh Framework Programme) to S.T. and A.B.

Data availability

Data are deposited in the Dryad Digital Repository (Brown et al., 2017): http://doi.org/10.5061/dryad.2538d

References

Airriess, C. N. and Childress, J. J. (1994). Homeoviscous properties implicated by the interactive effects of pressure and temperature on the hydrothermal vent crab *Bythograea thermydron*. *Biol. Bull.* **187**, 208-214.

Ashby, E. A. and Larimer, J. L. (1964). Cardiac responses of the crayfish, *Procambarus simulans*, to external and internal carbon dioxide stress. *Physiol. Zool.* **37**, 21-32.

Basse, A. L., Dixen, K., Yadav, R., Tygesen, M. P., Qvortrup, K., Kristiansen, K., Quistorff, B., Gupta, R., Wang, J. and Hansen, J. B. (2015). Global gene expression profiling of brown to white adipose tissue transformation in sheep reveals novel transcriptional components linked to adipose remodeling. *BMC Genom.* **16**, 215.

Benson, B. B. and Krause, D. (1984). The concentration and isotopic fractionation of oxygen dissolved in fresh-water and seawater in equilibrium with the atmosphere. *Limnol. Oceanogr.* **29**, 620-632.

Booth, C. E., McMahon, B. R. and Pinder, A. W. (1982). Oxygen uptake and the potentiating effects of increased hemolymph lactate on oxygen transport during exercise in the blue crab, *Callinectes sapidus*. *J. Comp. Physiol. B* **148**, 111-121.

Bracken-Grissom, H. D., Cannon, M. E., Cabezas, P., Feldmann, R. M., Schweitzer, C. E., Ahyong, S. T., Felder, D. L., Lemaitre, R. and Crandall, K. A. (2013). A comprehensive and integrative reconstruction of evolutionary history for Anomura (Crustacea: Decapoda). *BMC Evol. Biol.* **13**, 128.

Bridges, C. R. (2001). Modulation of haemocyanin oxygen affinity: properties and physiological implications in a changing world. *J. Exp. Biol.* **204**, 1021-1032.

Brown, A. and Thatje, S. (2014). Explaining bathymetric diversity patterns in marine benthic invertebrates and demersal fishes: physiological contributions to adaptation of life at depth. *Biol. Rev.* **89**, 406-426.

Brown, A. and Thatje, S. (2015). The effects of changing climate on faunal depth distributions determine winners and losers. *Glob. Change Biol.* **21**, 173-180.

Brown, J. H., Gillooly, J. F., Allen, A. P., Savage, V. M. and West, G. B. (2004). Toward a metabolic theory of ecology. *Ecology* **85**, 1771-1789.

Brown, A., Thatje, S., Morris, J. P., Oliphant, A., Morgan, E. A., Hauton, C., Jones, D. O. B. and Pond, D. W. (2017). Data from: Metabolic costs imposed by hydrostatic pressure constrain bathymetric range in the lithodid crab *Lithodes maja*. *Dryad Digital Repository* https://doi.org/10.5061/dryad.2538d.

Burnett, N. P., Seabra, R., De Pirro, M., Wethey, D. S., Woodin, S. A., Helmuth, B., Zippay, M. L., Sarà, G., Monaco, C. and Lima, F. P. (2013). An improved noninvasive method for measuring heartbeat of intertidal animals. *Limnol. Oceanogr. Methods* **11**, 91-100.

Bustin, S. A., Benes, V., Garson, J. A., Hellemans, J., Huggett, J., Kubista, M., Mueller, R., Nolan, T., Pfaffl, M. W., Shipley, G. L. et al. (2009). The MIQE guidelines: minimum information for publication of quantitative real-time PCR experiments. *Clin. Chem.* **55**, 611-622.

Campenot, R. B. (1975). The effects of high hydrostatic pressure on transmission at the crustacean neuromuscular junction. *Comp. Biochem. Physiol.* **52**, 133-140.

Christie, W. W. (1982). *Lipid Analysis: Isolation, Separation, Identification, and Structural Analysis of Lipids*. Oxford: Pergamon Press.

Cottin, D., Brown, A., Oliphant, A., Mestre, N. C., Ravaux, J., Shillito, B. Thatje, S. (2012). Sustained hydrostatic pressure tolerance of the shallow water shrimp *Palaemonetes varians* at different temperatures: insights into the colonisation of the deep sea. *Comp. Biochem. Physiol. A* **162**, 357-363.

Cramer, B. S., Miller, K. G., Barrett, P. J. and Wright, J. D. (2011). Late Cretaceous-Neogene trends in deep ocean temperature and continental ice volume: reconciling records of benthic foraminiferal geochemistry ($\delta^{18}O$ and Mg/Ca) with sea level history. *J. Geophys. Res.* **116**, C12023.

Deutsch, C., Ferrel, A., Seibel, B., Pörtner, H.-O. and Huey, R. B. (2015). Climate change tightens a metabolic constraint on marine habitats. *Science* **348**, 1132-1135.
Dingledine, R., Borges, K., Bowie, D. and Traynelis, S. F. (1999). The glutamate receptor ion channels. *Pharmacol. Rev.* **51**, 7-61.
Fehsenfeld, S. and Weihrauch, D. (2017). Acid-base regulation in aquatic decapod crustaceans. In *Acid-Base Balance and Nitrogen Excretion in Invertebrates* (ed. D. Weihrauch and M. O'Donnell), 151-191. Cham: Springer.
Folch, J., Lees, M. and Stanley, G. H. S. (1957). A simple method for the isolation and purification of total lipides from animal tissue. *J. Biol. Chem.* **226**, 497-509.
Frederich, M. and Pörtner, H. O. (2000). Oxygen limitation of thermal tolerance defined by cardiac and ventilatory performance in spider crab, *Maja squinado*. *Am. J. Physiol. Reg. Integr.Comp. Physiol.* **279**, R1531-R1538.
George, R. Y. (1984). Ontogenetic adaptations in growth and respiration of *Euphausia superba* in relation to temperature and pressure. *J. Crust. Biol.* **4**, 252-262.
Gerringer, M. E., Drazen, J. C. and Yancey, P. H. (2017). Metabolic enzyme activities of abyssal and hadal fishes: pressure effects and a re-evaluation of depth-related changes. *Deep-Sea Res. I* **125**, 135-146.
Glazier, D. S. (2005). Beyond the '3/4-power law': variation in the intra- and interspecific scaling of metabolic rate in animals. *Biol. Rev.* **80**, 611-662.
Goldenthal, M. J., Marin-Garcia, J. and Ananthakrishnan, R. (1998). Cloning and molecular analysis of the human citrate synthase gene. *Genome* **41**, 733-738.
Hall, S. and Thatje, S. (2009). Global bottlenecks in the distribution of marine Crustacea: temperature constraints in the family Lithodidae. *J. Biogeogr.* **36**, 2125-2135.
Hazel, J. R. (1995). Thermal adaptation in biological membranes: is homeoviscous adaptation the explanation? *Ann. Rev. Physiol.* **57**, 19-42.
Hazel, J. R. and Williams, E. E. (1990). The role of alterations in membrane lipid composition in enabling physiological adaptation of organisms to their physical environment. *Prog. Lipid Res.* **29**, 167-227.
Hepp, Y., Tano, M. C., Pedreira, M. E. and Freudenthal, R. A. M. (2013). NMDA-like receptors in the nervous system of the crab *Neohelice granulata*: A neuroanatomical description. *J. Comp. Neurol.* **521**, 2279-2297.
Hill, A. D., Taylor, A. C. and Strang, R. H. C. (1991). Physiological and metabolic responses of the shore crab *Carcinus maenas* (L.) during environmental anoxia and subsequent recovery. *J. Exp. Mar. Biol. Ecol.* **150**, 31-50.
Hofmann, A. F., Peltzer, E. T. and Brewer, P. G. (2013a). Kinetic bottlenecks to chemical exchange rates for deep-sea animals – Part 2: Carbon dioxide. *Biogeosci.* **10**, 2409-2425.
Hofmann, A. F., Peltzer, E. T. and Brewer, P. G. (2013b). Kinetic bottlenecks to respiratory exchange rates in the deep-sea – Part 1: Oxygen. *Biogeosci.* **10**, 5049-5060.
Jones, D. O. B., Yool, A., Wei, C.-L., Henson, S. A., Ruhl, H. A., Watson, R. A. and Gehlen, M. (2014). Global reductions in seafloor biomass in response to climate change. *Glob. Change Biol.* **20**, 1861-1872.
Kassahn, K. S., Crozier, R. H., Pörtner, H. O. and Caley, M. J. (2009). Animal performance and stress: responses and tolerance limits at different levels of biological organisation. *Biol. Rev.* **84**, 277-292.
Kooijman, S. A. L. M. (2010). *Dynamic Energy Budget Theory for Metabolic Organisation*. Cambridge: Cambridge University Press.
Macpherson, E. (1988). Revision of the family Lithodidae Samouelle, 1819 (Crustacea, Decapoda, Anomura) in the Atlantic Ocean. *Monogr. Zool. Mar.* **2**, 9-153.
Madeira, D., Narciso, L., Cabral, H. N., Diniz, M. S. and Vinagre, C. (2012). Thermal tolerance of the crab *Pachygrapsus marmoratus*: intraspecific differences at a physiological (CTMax) and molecular level (Hsp70). *Cell Stress Chaper.* **17**, 707-716.
McMahon, B. R. (1999). Intrinsic and extrinsic influences on cardiac rhythms in crustaceans. *Comp. Biochem. Physiol. A* **124**, 539-547.
McMahon, B. R. (2001). Respiratory and circulatory compensation to hypoxia in crustaceans. *Resp. Physiol.* **128**, 349-364.
Mickel, T. J. and Childress, J. J. (1982a). Effects of pressure and temperature on the EKG and heart rate of the hydrothermal vent crab *Bythograea thermydron* (Brachyura). *Biol. Bull.* **162**, 70-82.
Mickel, T. J. and Childress, J. J. (1982b). Effects of temperature, pressure, and oxygen concentration on the oxygen consumption rate of the hydrothermal vent crab *Bythograea thermydron* (Brachyura). *Physiol. Zool.* **55**, 199-207.
Mor, A. and Grossman, Y. (2010). The efficacy of physiological and pharmacological N-methyl-D-aspartate receptor block is greatly reduced under hyperbaric conditions. *Neuroscience* **169**, 1-7.
Morris, J. P., Thatje, S. and Hauton, C. (2013). The use of stress-70 proteins in physiology: a re-appraisal. *Mol. Ecol.* **22**, 1494-1502.
Morris, J. P., Thatje, S., Cottin, D., Oliphant, A., Brown, A., Shillito, B., Ravaux, J. and Hauton, C. (2015a). The potential for climate-driven bathymetric range shifts: sustained temperature and pressure exposures on a marine ectotherm, *Palaemonetes varians*. *R. Soc. Open Sci.* **2**, 150472.
Morris, J. P., Thatje, S., Ravaux, J., Shillito, B., Fernando, D. and Hauton, C. (2015b). Acute combined pressure and temperature exposures on a shallow-water crustacean: Novel insights into the stress response and high pressure neurological syndrome. *Comp. Biochem. Physiol. A* **181**, 9-17.
Morris, J. P., Thatje, S., Ravaux, J., Shillito, B. and Hauton, C. (2015c). Characterising multi-level effects of an acute pressure exposure on a shallow-water invertebrate: insights into the kinetics and hierarchy of the stress response. *J. Exp. Biol.* **218**, 2594-2602.
Munro, C., Morris, J. P., Brown, A., Hauton, C. and Thatje, S. (2015). The role of ontogeny in physiological tolerance: Decreasing hydrostatic pressure tolerance with development in the northern stone crab *Lithodes maja*. *Proc. R. Soc. B* **282**, 20150577.
New, P., Brown, A., Oliphant, A., Burchell, P., Smith, A. and Thatje, S. (2014). The effects of temperature and pressure acclimation on the temperature and pressure tolerance of the shallow-water shrimp *Palaemonetes varians*. *Mar. Biol.* **161**, 697-709.
Nogales, E. (2000). Structural insights into microtubule function. *Ann. Rev. Biochem.* **69**, 277-302.
OBIS (2016). *Data from the Ocean Biogeographic Information System*. Intergovernmental Oceanographic Commission of UNESCO.
Picard, A. and Daniel, I. (2013). Pressure as an environmental parameter for microbial life – a review. *Biophys. Chem.* **183**, 30-41.
Pinsky, M. L., Worm, B., Fogarty, M. J., Sarmiento, J. L. and Levin, S. A. (2013). Marine taxa track local climate velocities. *Science* **341**, 1239-1242.
Pond, D. W., Tarling, G. A. and Mayor, D. J. (2014). Hydrostatic pressure and temperature effects on the membranes of a seasonally migrating marine copepod. *PLoS ONE*, **9**, e111043.
Pörtner, H. O. (2002). Climate variations and the physiological basis of temperature dependent biogeography: Systemic to molecular hierarchy of thermal tolerance in animals. *Comp. Biochem. Physiol. A* **132**, 739-761.
Pörtner, H.-O. (2010). Oxygen- and capacity-limitation of thermal tolerance: a matrix for integrating climate-related stressor effects in marine ecosystems. *J. Exp. Biol.* **213**, 881-893.
Pörtner, H. O. and Farrell, A. P. (2008). Physiology and climate change. *Science* **322**, 690-692.
Robinson, N. J., Thatje, S. and Osseforth, C. (2009). Heartbeat sensors under pressure: a new method for assessing hyperbaric physiology. *High Press. Res.* **29**, 422-430.
Ryan, T. J. and Grant, S. G. N. (2009). The origin and evolution of synapses. *Nat. Rev. Neurosci.* **10**, 701-712.
Sébert, P. (2010). *Comparative High Pressure Biology*. Enfield: Science Publishers.
Shillito, B., Gaill, F. and Ravaux, J. (2014). The IPOCAMP pressure incubator for deep-sea fauna. *J. Mar. Sci. Technol.* **22**, 97-102.
Sibly, R. M., Brown, J. H. and Kodric-Brown, A. (2012). *Metabolic Ecology: A Scaling Approach*. Chichester: Wiley-Blackwell.
Snow, S. (2010). The evolutionary history and phylogeny of the Lithodinae (Decapoda: Anomura: Lithodidae). *PhD thesis*, University of Southampton.
Sokolova, I. M. (2013). Energy-limited tolerance to stress as a conceptual framework to integrate the effects of multiple stressors. *Integr. Comp. Biol.* **53**, 597-608.
Somero, G. N. (1992). Adaptations to high hydrostatic pressure. *Annu. Rev. Physiol.* **54**, 557-577.
Stager, M., Swanson, D. L. and Cheviron, Z. A. (2015). Regulatory mechanisms of metabolic flexibility in the dark-eyed junco (*Junco hyemalis*). *J. Exp. Biol.* **218**, 767-777.
Thatje, S. and Robinson, N. J. (2011). Specific dynamic action affects the hydrostatic pressure tolerance of the shallow-water spider crab *Maja brachydactyla*. *Naturwissenschaften* **98**, 299-313.
Vaquer-Sunyer, R. and Duarte, C. M. (2008). Thresholds of hypoxia for marine biodiversity. *Proc. Natl. Acad. Sci. USA* **105**, 15452-15457.
Vinuesa, J. H. (1984). Sistema reproductor, ciclo y madurez gonadal de la centolla (*Lithodes antarcticus*) del canal Beagle. *Mar del Plata* **441**, 241-246.
West, G. B. and Brown, J. H. (2005). The origin of allometric scaling laws in biology from genomes to ecosystems: Towards a quantitative unifying theory of biological structure and organization. *J. Exp. Biol.* **208**, 1575-1592.
Wheatly, M. G. and Taylor, E. W. (1981). The effect of progressive hypoxia on heart rate, ventilation, respiratory gas exchange and acid-base status in the crayfish *Austropotamobius pallipes*. *J. Exp. Biol.* **92**, 125-141.
Wilkens, J. L. (1999). The control of cardiac rhythmicity and of blood distribution in crustaceans. *Comp. Biochem. Physiol. A* **124**, 531-538.
Willmer, P., Stone, G. and Johnston, I. A. (2005). *Environmental Physiology of Animals*. Malden: Wiley-Blackwell.
Withers, P. C. (1992). *Comparative Animal Physiology*. Fort Worth: Saunders College Publishing.
Woolley, S. N. C., Tittensor, D. P., Dunstan, P. K., Guillera-Arroita, G., Lahoz-Monfort, J. J., Wintle, B. A., Worm, B. and O'Hara, T. D. (2016). Deep-sea diversity patterns are shaped by energy availability. *Nature* **533**, 393-396.
Zaklan, S. D. (2002). Review of the family Lithodidae (Crustacea: Anomura: Paguroidea): distribution, biology, and fisheries. In *Crabs in Cold Water Regions: Biology, Management, and Economics* (ed. A. J. Paul, E. G. Dawe, R. Elner, G. S. Jamieson, G. H. Kruse, R. S. Otto, B. Sainte-Marie, B. Shirley and D. Woodby), pp. 751-845. Fairbanks: Alaska Sea Grant College Program.

Journal of Experimental Biology